

Essence of Shock Capturing

Taku Ohwada* and Taichi Nakamura

Department of Aeronautics and Astronautics, Graduate School of Engineering,
Kyoto University

Abstract

The numerical flux of the kinetic Lax-Wendroff scheme [J. Comput. Phys. **211** 424-447 (2006) & J. Comput. Phys. **255** 106-129 (2013)] comprises three parts: a dissipative one (that of the equilibrium flux method), a less dissipative one, and the one corresponding to the time derivative of the flux vector. The formula of the numerical flux is expressed in terms of averages with a common structure, which is slightly different from the standard form for shock capturing. In the present article these averages are simplified and are modified in order to elucidate key structures of numerical dissipation for shock/boundary-layer/contact-discontinuity capturing.

1 INTRODUCTION

A gas is highly nonequilibrium inside a nonweak shock wave. Its thickness is of the order of the mean free path of gas molecules (about 10^{-7} meter under standard conditions for temperature and pressure), which is usually far smaller than the characteristic length of the flow, such as the size of a vehicle. Shock capturing is a numerical technique for continuum gas-dynamic equations and it aims to capture a shock wave within a few mesh intervals without the violation of the second law of thermodynamics and the presence of spurious oscillations. Its nature is still compromising or conciliatory despite the long history of its study. Its rationality, however, is not lost at all even nowadays, when computer technology has been significantly developed and the necessity of multi-scale analyses is loudly claimed in many fields of science and technology.¹

The main building blocks of modern shock-capturing schemes are the reconstruction of distributions of gas-dynamic variables from their discrete data, such as MUSCL, ENO, and WENO, and the numerical flux, such as HLL's and AUSM's, and they are like the body and the engine of an automobile. Although these modern technologies are recognized as indispensable tools for complex supersonic flow simulations, however, it is an undeniable fact that the status of the modern shock capturing is far away from excellence. For example, even the HLLE scheme [2, 1] and the Rusanov scheme [14] (local Lax-Friedrichs), the robustness of which is highly appreciated among experts, cannot escape shock anomalies, such as carbuncle phenomenon and post-shock oscillations, which frequently arise in hypersonic flow simulations and considerably deteriorate the reliability of the outcomes, such as the prediction of aerodynamic force and heating. Although numerical dissipation (additive or intrinsic) is a key to the fix, however, it is a double-edged sword. A small dose of it considerably smears boundary layers, which are formed by very small *physical* dissipation, and contact discontinuities, which are without self-sharpening mechanism. Desired are schemes which combine strong resistance against shock anomalies and low diffusive behavior in a region away from shock waves. The goal of shock capturing is not achieved only by sophistication of the body. Persistent upgrade of the engine, which the present article mainly concerns, is also needed.

Kinetic schemes have been attracting interests because of their robustness. In particular, the equilibrium flux method (EFM) [11], which is one of the origins of kinetic schemes, is nearly free from shock anomalies when the spatial accuracy is restricted to first order. Because of its very dissipative nature, however, it cannot capture boundary-layers with rational resolutions. This

*Corresponding author: ohwada@kuaero.kyoto-u.ac.jp

¹The Kolmogorov scale is much larger than the mean free path [5] and the usefulness of shock capturing is confirmed even for flows with the smallest macroscopic scale.[3]

drawback is not resolved only by the introduction of second order accurate reconstruction, such as MUSCL, while a classical central scheme of second order accuracy suffices for boundary-layer capturing. Both shock-capturing and boundary-layer capturing are established in the kinetic scheme of Refs. [8, 9], which is called in the present article the kinetic Lax-Wendroff scheme (KLW). The numerical flux of KLW comprises that of EFM, a less dissipative one, and the one corresponding to the time derivative of the flux vector. KLW is operated in such a way that it changes towards the 1st order accurate EFM around shock waves and the Lax-Wendroff scheme away from them. The gas kinetic BGK scheme [17] can also be regarded as a hybrid scheme of EFM and a less dissipative kinetic scheme and the allocation is controlled in a way similar to KLW. Although these kinetic schemes are equipped with sufficiently high robustness for usual supersonic flow simulations, however, their original directions are not sufficient for the prevention and suppression of shock anomalies, especially under severe conditions. A simple remedy at the preprocessing level, which enhances the transformation towards the 1st order accurate EFM around shock waves, drastically improves the resistance against shock anomalies in exchange for a slight increase in thickness of the numerically captured shock wave [9].

Kinetic schemes have developed into the practical level but there still remains an academic question about the essence; even the numerical fluxes of kinetic schemes are expressed in terms of macroscopic variables. In order to elucidate it, we will simplify KLW without decrease in performance. Sharp contact-discontinuity capturing is one of the noteworthy properties of the Riemann solver approach, such as the exact Riemann solver, Osher-Solomon [10], and HLLC [16]. This property will be shown to be established only by a simple modification of the numerical dissipation of KLW.

2 FORMULAS OF SIMPLIFIED KLW

2.1 Assumption and notation

The gas under consideration is assumed to be ideal for brevity of explanation. Time and Cartesian space coordinates are denoted by t and (x, y) , respectively. The density, the components of the flow velocity in the x and y directions, and the pressure of the gas are denoted by ρ , u , v , and P , respectively. These gas-dynamic variables, called the primitive variables, are often denoted by the vector $\mathbf{h} = (\rho, u, v, P)^T$ for concise expression. The conservative variables, which are defined by $(\rho, \rho u, \rho v, \rho(u^2 + v^2)/2 + P/(\gamma - 1))^T$ (γ is the heat capacity ratio), are denoted by the vector $\tilde{\mathbf{h}}$. The temperature of the gas is denoted by T , which is defined by the EOS, i.e. $T = P/\rho$. Incidentally, the explanation below can be read as that with the dimensional variables if T is regarded as RT (R is the gas constant per unit mass).

2.2 Basic equations

The 2D compressible Euler equations are written in the form:

$$\frac{\partial \tilde{\mathbf{h}}}{\partial t} + \frac{\partial \Phi}{\partial x} + \frac{\partial \Psi}{\partial y} = 0, \quad (1)$$

where Φ and Ψ are the flux vectors defined by

$$\Phi = \begin{pmatrix} \rho u \\ \rho u^2 + P \\ \rho uv \\ [\frac{\gamma P}{\gamma - 1} + \rho \frac{u^2 + v^2}{2}]u \end{pmatrix}, \quad (2)$$

$$\Psi = \begin{pmatrix} \rho v \\ \rho uv \\ \rho v^2 + P \\ [\frac{\gamma P}{\gamma - 1} + \rho \frac{u^2 + v^2}{2}]v \end{pmatrix}. \quad (3)$$

2.3 Numerical flux

The derivation of KLW is explained in Refs. [8, 9]. KLW is categorized into the finite volume method and its temporal accuracy is formally second order. Owing to the invariance of the gas-dynamic equation system under rotation of a coordinate system, it suffices to consider a cell-edge with its unit normal in the direction of x .

The numerical flux for the time step Δt and the unit length is defined by

$$\mathcal{F} = \int_0^{\Delta t} \Phi(\mathbf{h}(t, \dots)) dt. \quad (4)$$

The numerical flux of KLW is expressed in the form:

$$\mathcal{F} = \Delta t (\alpha \mathbf{F}^D + (1 - \alpha) \mathbf{F}^C) + \frac{(\Delta t)^2}{2} \Phi_t. \quad (5)$$

The \mathbf{F}^D is the numerical flux of EFM, \mathbf{F}^C is a less dissipative one, and Φ_t corresponds to $\partial\Phi/\partial t$. It suffices for the 2nd order spatial accuracy to compute \mathcal{F} at the middle point of the cell-edge (or its vicinities). This point is assumed to be located at the origin of the coordinates $(x, y) = (0, 0)$. The \mathbf{F}^D , \mathbf{F}^C , and Φ_t are computed from the limiting values of \mathbf{h} and $\partial\mathbf{h}/\partial s$ ($s = x, y$) at both sides of the cell-edge:

$$\mathbf{h}^L = \lim_{x \rightarrow 0^-} \mathbf{h}(x, y = 0, t = 0), \quad \mathbf{h}^R = \lim_{x \rightarrow 0^+} \mathbf{h}(x, y = 0, t = 0), \quad (6)$$

$$\mathbf{h}_s^L = \lim_{x \rightarrow 0^-} \frac{\partial \mathbf{h}}{\partial s}(x, y = 0, t = 0), \quad \mathbf{h}_s^R = \lim_{x \rightarrow 0^+} \frac{\partial \mathbf{h}}{\partial s}(x, y = 0, t = 0) \quad (s = x, y). \quad (7)$$

These data are supplied by MUSCL reconstruction, the formal accuracy of which is second order. The value of the parameter α ranges from 0 to 1. We prefer to compute it from the pressure jump at the cell-edge by using the formula

$$\alpha = 1 - \exp(-C \frac{|P^L - P^R|}{P^L + P^R}), \quad (8)$$

where C is an empirical positive constant; $C = 10$ in the present article. The guiding principle of this *clutch* is that \mathbf{F}^D becomes dominant around shock waves and vice versa in a region away from them.

The explicit expression of \mathbf{F}^D is given by²

$$\mathbf{F}^D = \left(\frac{1 + a^L}{2} \Phi^L + \frac{1 - a^R}{2} \Phi^R \right) + (b^L \tilde{\mathbf{h}}^L - b^R \tilde{\mathbf{h}}^R), \quad (9)$$

where

$$\Phi^H = \Phi(\mathbf{h}^H) \quad (H = L, R), \quad (10)$$

$$a^H = A\left(\frac{u^H}{\sqrt{2T^H}}\right) \quad (H = L, R), \quad (11)$$

$$b^H = \sqrt{\frac{T^H}{2\pi}} B\left(\frac{u^H}{\sqrt{2T^H}}\right) \quad (H = L, R), \quad (12)$$

$$A(m) = \operatorname{erf}(m), \quad B(m) = \exp(-m^2). \quad (13)$$

²Equation (13) is the consequence of the fact that the Maxwell distribution function is employed in the derivation. Non-orthodox functions, such as

$$A(m) = \frac{m + 4m^3}{1 + |m + 4m^3|},$$

$$B(m) = \frac{m^2 + 2}{6m^4 + 2m^2 + 2},$$

can be employed safely.

In the case of the original KLW, \tilde{h}^H in the second bracket on the right hand side of Eq. (9) is replaced by $\tilde{h}^H + (0, 0, 0, P^H/2)^T$. The formula of the modified F^D is regarded as an extension of the standard form of numerical flux for shock capturing:

$$F^D = \left(\frac{1+a}{2} \Phi^L + \frac{1-a}{2} \Phi^R \right) + b(\tilde{h}^L - \tilde{h}^R). \quad (14)$$

The formula of the modified F^D becomes the standard type for $u^L = u^R = u_*$ and $T^L = T^R = T_*$, where u_* and T_* are defined appropriately, e.g.

$$u_* = \frac{u^L + u^R}{2}, \quad T_* = \frac{T^L + T^R}{2}. \quad (15)$$

The standard-type numerical flux becomes an upwind approximation of the flux vector without dissipative term for $|u_*/\sqrt{T_*}| \gg 1$ ($\lim_{m \rightarrow \infty} B(m) = 0$) and a central one with dissipative term for $u = 0$ ($B(0) = 1$). The standard-type scheme so constructed works as a shock capturing scheme but it is not robust against strong rarefaction waves; the stability is enhanced by the separation $a \rightarrow (a^L, a^R)$ and $b \rightarrow (b^L, b^R)$. Incidentally, the Rusanov scheme is well known as one of the robust shock capturing schemes. Its numerical flux is the standard type ($a = 0$ and $b = |u| + c$; c is the speed of sound). Although it is more diffusive than EFM judging from the thickness of numerically captured shock, it is less robust than EFM; post-shock oscillations produced by the Rusanov scheme are many orders of magnitude larger than those in the case of EFM.

The F^C is defined by

$$F^C = \Phi(h^C), \quad (16)$$

where the primitive variables h^C are computed from the conservative variables \tilde{h}^C . In the original KLW, \tilde{h}^C is defined by

$$\tilde{h}^C = \frac{1+a^L}{2} \tilde{h}^L + \frac{1-a^R}{2} \tilde{h}^R + b^L d^L - b^R d^R, \quad (17)$$

$$d^H = (0, \rho^H, 0, \rho^H u^H/2)^T \quad (H = L, R). \quad (18)$$

In the simplified KLW, h^C is computed according to the following formulas:

$$\begin{aligned} \begin{pmatrix} \rho^C \\ (\rho u)^C \\ (\rho v)^C \end{pmatrix} &= \frac{1+a^L}{2} \begin{pmatrix} \rho^L \\ \rho^L u^L \\ \rho^L v^L \end{pmatrix} + \frac{1-a^R}{2} \begin{pmatrix} \rho^R \\ \rho^R u^R \\ \rho^R v^R \end{pmatrix} \\ &+ b_*^L \begin{pmatrix} 0 \\ P^L/T_* \\ 0 \end{pmatrix} - b_*^R \begin{pmatrix} 0 \\ P^R/T_* \\ 0 \end{pmatrix}, \end{aligned} \quad (19)$$

$$u^C = (\rho u)^C / \rho^C, \quad v^C = (\rho v)^C / \rho^C, \quad (20)$$

$$P^C = \frac{1+a_*^L}{2} P^L + \frac{1-a_*^R}{2} P^R, \quad (21)$$

where

$$a_*^H = A \left(\frac{u^H}{\sqrt{2T_*}} \right) \quad (H = L, R), \quad (22)$$

$$b_*^H = \sqrt{\frac{T_*}{2\pi}} B \left(\frac{u^H}{\sqrt{2T_*}} \right) \quad (H = L, R). \quad (23)$$

The Φ_t , which corresponds to

$$\frac{\partial \Phi}{\partial t} = \frac{\partial \Phi}{\partial \tilde{h}} \frac{\partial \tilde{h}}{\partial t} = -\frac{\partial \Phi}{\partial \tilde{h}} \left(\frac{\partial \Phi}{\partial x} + \frac{\partial \Psi}{\partial y} \right),$$

is defined by

$$\Phi_t = -L^C (\Delta \Phi + \Delta \Psi), \quad (24)$$

$$\Delta\Phi = \left(\frac{1+a^L}{2} M^L \mathbf{h}_x^L + \frac{1-a^R}{2} M^R \mathbf{h}_x^R \right) + (b^L \mathbf{W}^L \mathbf{h}_x^L - b^R \mathbf{W}^R \mathbf{h}_x^R), \quad (25)$$

$$\Delta\Psi = \left(\frac{1+a^L}{2} N^L \mathbf{h}_y^L + \frac{1-a^R}{2} N^R \mathbf{h}_y^R \right) + (b^L \mathbf{Z}^L \mathbf{h}_y^L - b^R \mathbf{Z}^R \mathbf{h}_y^R), \quad (26)$$

where L^C , M^H , N^H , W^H , and Z^H are $L(\mathbf{h}^C)$, $M(\mathbf{h}^H)$, $N(\mathbf{h}^H)$, $W(\mathbf{h}^H)$, and $Z(\mathbf{h}^H)$ ($H = L, R$), respectively, and $L(\mathbf{h})$, $M(\mathbf{h})$, $N(\mathbf{h})$, $W(\mathbf{h})$, and $Z(\mathbf{h})$ are 4×4 matrices. In the original KLW, they are defined by

$$L(\mathbf{h}) = \begin{pmatrix} 0 & 1 & 0 & 0 \\ \frac{(\gamma-3)u^2 + (\gamma-1)v^2}{2} & (3-\gamma)u & (1-\gamma)v & \gamma-1 \\ -uv & v & u & 0 \\ u \left(\frac{(\gamma-2)(u^2+v^2)}{2} - \frac{\gamma P}{(\gamma-1)\rho} \right) & \frac{(3-2\gamma)u^2+v^2}{2} + \frac{\gamma P}{(\gamma-1)\rho} & (1-\gamma)uv & \gamma u \end{pmatrix}, \quad (27)$$

$$M(\mathbf{h}) = \begin{pmatrix} u & \rho & 0 & 0 \\ u^2 & 2\rho u & 0 & 1 \\ uv & \rho v & \rho u & 0 \\ u \frac{u^2+v^2}{2} & \rho \frac{3u^2+v^2}{2} + \frac{\gamma P}{\gamma-1} & \rho uv & \frac{\gamma u}{\gamma-1} \end{pmatrix}, \quad (28)$$

$$N(\mathbf{h}) = \begin{pmatrix} v & 0 & \rho & 0 \\ uv & \rho v & \rho u & 0 \\ v^2 & 0 & 2\rho v & 1 \\ v \frac{u^2+v^2}{2} & \rho uv & \rho \frac{u^2+3v^2}{2} + \frac{\gamma P}{\gamma-1} & \frac{\gamma v}{\gamma-1} \end{pmatrix}, \quad (29)$$

$$W(\mathbf{h}) = \begin{pmatrix} \frac{1}{2} & 0 & 0 & \frac{\rho}{2P} \\ u & 2\rho & 0 & 0 \\ \frac{v}{2} & 0 & \rho & \frac{\rho v}{2P} \\ \frac{1}{4} \left(2u^2 + v^2 - \frac{(\gamma+1)P}{(\gamma-1)\rho} \right) & \frac{3\rho u}{2} & \rho v & \frac{1}{4} \left(\frac{\rho v^2}{P} + \frac{3(\gamma+1)}{\gamma-1} \right) \end{pmatrix}, \quad (30)$$

and

$$Z(\mathbf{h}) = \begin{pmatrix} \frac{\rho uv}{2P} & \frac{\rho^2 v}{P} & 0 & -\frac{\rho^2 uv}{2P^2} \\ \frac{v}{2} & 0 & \rho & \frac{\rho v}{2P} \\ \frac{u}{2} \left(\frac{\rho v^2}{P} + 1 \right) & \rho \left(\frac{\rho v^2}{P} + 1 \right) & 0 & -\frac{\rho u}{2P} \left(\frac{\rho v^2}{P} + 1 \right) \\ \frac{uv}{4} \left(\frac{\rho v^2}{P} + \frac{3\gamma-1}{\gamma-1} \right) & \frac{\rho v}{2} \left(\frac{\rho v^2}{P} + \frac{3\gamma-1}{\gamma-1} \right) & \frac{\rho u}{2} & -\frac{\rho uv}{4P} \left(\frac{\rho v^2}{P} + \frac{\gamma+1}{\gamma-1} \right) \end{pmatrix}. \quad (31)$$

The matrices L , M , and N correspond to $\partial\Phi/\partial\tilde{\mathbf{h}}$, $\partial\Phi/\partial\mathbf{h}$, and $\partial\Psi/\partial\mathbf{h}$, respectively, and $\Delta\Phi$ and $\Delta\Psi$ approximate $\partial\Phi/\partial x$ and $\partial\Psi/\partial y$, respectively. The first bracket on the right hand side of Eq. (25) gives a weighted average of $(\partial\Phi/\partial x)^L$ and $(\partial\Phi/\partial x)^R$ and the first bracket on the right hand side of Eq. (26) does that of $(\partial\Psi/\partial y)^L$ and $(\partial\Psi/\partial y)^R$. The second bracket on the right hand side of Eq. (25) and that of Eq. (26) are expected to yield some kind of numerical dissipation. In the simplified KLW, the matrices W and Z are replaced by

$$W(\mathbf{h}) = Z(\mathbf{h}) = \mathbf{O}, \quad (32)$$

or

$$\mathbf{W}(\mathbf{h}) = \begin{pmatrix} 0 & 0 & 0 & \frac{\rho}{2P} \\ 0 & 2\rho & 0 & 0 \\ 0 & 0 & 0 & \frac{\rho v}{2P} \\ 0 & \frac{3\rho u}{2} & 0 & \frac{1}{4}\left(\frac{\rho v^2}{P} + \frac{3(\gamma+1)}{\gamma-1}\right) \end{pmatrix}, \quad \mathbf{Z}(\mathbf{h}) = \mathbf{O}. \quad (33)$$

The simplified KLW with Eq. (32) and that with Eq. (33) will be hereafter called KLWC and KLWC2, respectively.

The modification of \mathbf{F}^C and Φ_t is for sharp capturing of stationary contact-discontinuities. Suppose a flow field satisfying $u \equiv 0$ and $P \equiv P_0 (= \text{Const.})$ in the neighborhood of a stationary contact discontinuity. The value of the parameter α is zero and \mathbf{F}^D does not contribute to the numerical flux at cell-edges in the neighborhood of the contact discontinuity, i.e. Eq. (8) with $P^L = P^R$. The modified formulas of \mathbf{F}^C and Φ_t yield $\mathbf{F}^C = (0, P_0, 0, 0)$ and $\Phi_t = (0, 0, 0, 0)$ there irrespective of the distributions of ρ and v . Then the contact discontinuity is kept as it is, which is the simple consequence of the balance of numerical fluxes. Although \mathbf{F}^C is less dissipative than \mathbf{F}^D , its numerical dissipation is needed for shock capturing.³ The main point of the modification is that numerical dissipation necessary for shock capturing is retained. The compatibility between shock capturing and sharp contact-discontinuity capturing can also be made by the conventional Riemann solver approach, such as HLLC. Our claim is that it can be made only by a treatment of numerical dissipation. Numerical dissipation is also needed in Φ_t for shock capturing.⁴ In fact, KLWC, i.e. Eq. (32), exhibits small but appreciable oscillatory behavior around a stationary shock wave. This can be fixed if the computation is done together with the remedy against shock anomalies proposed in Ref. [9].

3 NUMERICAL EXAMPLES

Figure 1 shows the density distributions of the steady flow field with a contact discontinuity

$$(\rho, u, v, P) = \begin{cases} (10 + \sin 5\pi x, 0, 1 + \sin 5\pi x, 1) & x < 0 \\ (1 - \frac{1}{2}\sin 5\pi x, 0, -\frac{1}{2} - \sin 5\pi x, 1) & x > 0 \end{cases}. \quad (34)$$

This flow field is employed as the initial condition and the snapshots at $t = 2$ are shown in the figure. The flow field is kept as it is in the computations of HLLC, KLWC, KLWC2; the results of KLWC and KLWC2 with the remedy against shock anomalies, i.e. KLWCR and KLWC2R, which are identical to those of KLWC and KLWC2, are shown in the figure. In contrast, the result of KLW is slightly diffusive. The flow field is heavily deteriorated in the computations of Rusanov and HLLC.

Figure 2 shows the density isolines for $M=8.1$ viscous flow past a cylinder; the Reynolds number is 1.3×10^5 . KLW, KLWC, and KLWC2 with the remedy against shock anomalies (KLWR, KLWCR, KLWC2R) yield almost identical results. Incidentally, HLLC and HLLC exhibit shock anomalies even in their 1st order accurate computations (no figure). The temperature distribution along the axis of symmetry is depicted for different mesh systems and different resolutions in Fig. 3. The boundary-layer is captured well even with the lowest resolution (10 points in the layer).

4 CONCLUDING REMARKS

There remains essentially no kinetic ingredient in KLWC and KLWC2. Nevertheless the performance is identical to or higher than the original KLW. MUSCL was employed in the computations

³Spurious oscillations arise if \mathbf{F}^C is computed from $\mathbf{h}^C = (\mathbf{h}^L + \mathbf{h}^R)/2$.

⁴KLW is regarded as an extension of the Lax-Wendroff scheme, which is second order accurate in time, and KLW can also be modified as an extension of the two-step version, which is without the term Φ_t ; the numerical flux at $t = \Delta t/2$ is computed from \mathbf{h} at $t = \Delta t/2$, which is computed from that at $t = 0$ by the first order accurate formula. The two-step version of the simplified KLW, where only the formulas of \mathbf{F}^D and \mathbf{F}^C are needed, exhibits performance identical to its single step version with the time derivative term.

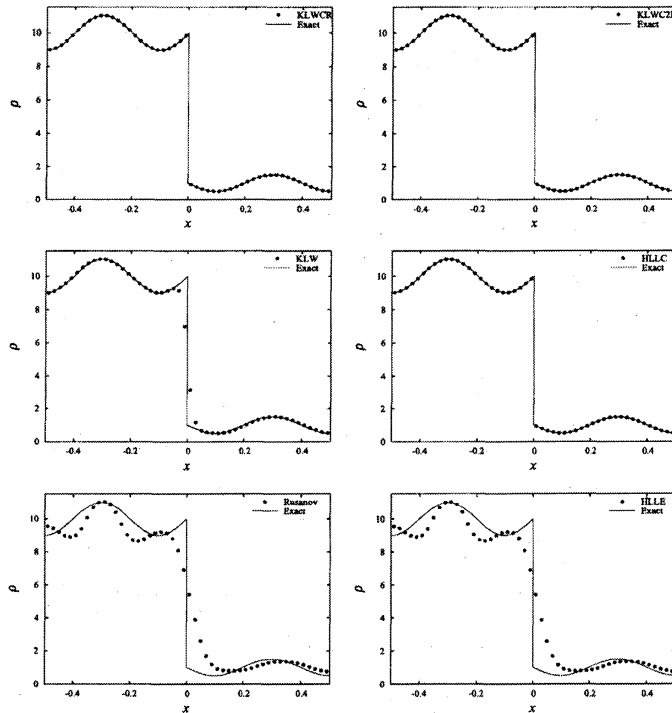


Figure 1: Density distribution around a stationary contact discontinuity.

of the present article. The employment of WENO, which is a more sophisticated reconstruction technique with higher order accuracy, is considered as an extension. However, the combination of KLW and WENO does not bring about the improvement. On the contrary, it causes an unacceptable behavior of the numerical solution around shock waves. WENO scheme with Rusanov numerical flux is now widely employed as a successful high order accurate shock capturing scheme, however, it exhibits an anomalous behavior in hypersonic flow regime.[15]. The study on the compatibility between high order accuracy for smooth solutions and strong resistance against shock anomalies is underway.

John von Neumann and Robert Richtmyer published a milestone paper [7] in 1950, which had been serving until 1993 as the official document for proof of the first introduction of artificial dissipative terms into gas-dynamic equations for shock capturing.⁵ Various methods for shock capturing have been proposed since their pioneering work. As demonstrated in the present article, shock/boundary-layer/contact-discontinuity capturing is established only by treatment of numerical dissipation and its control. Modern studies on shock capturing are still empirical no matter how they look theoretical because of the lack of mathematical theory of numerical methods for nonlinear systems of conservation laws. In this somewhat radical view, the Riemann solver approach as well as the Boltzmann (kinetic) one is merely a classy expedient and there is no need for hesitating to go back to von Neumann and Richtmyer, or more specifically, Richtmyer, in the early days of shock-capturing schemes. Richtmyer's two technical reports in 1948 [12, 13], which had been classified until 1993 without any rational reason, are now serving as the oldest official documents for proof of the first introduction of artificial dissipative terms into gas-dynamic equations for shock capturing. He described "artificial dissipative terms" as "*mock* dissipative terms" in the abstract of the second technical report, or more precisely, "*mock*" was replaced by the more sophisticated expression "artificial" in the subsequent academic journal paper [7]. The approach to shock capturing in the present article is regarded as engineering rather than mathematical or physical. Its usefulness is supported by the essence of shock capturing, which was already summed up in Richtmyer's unashamed and frank word in 1948.

⁵The interested reader is referred to e.g. Ref. [4] and references therein for the history of shock-capturing schemes in the early days.

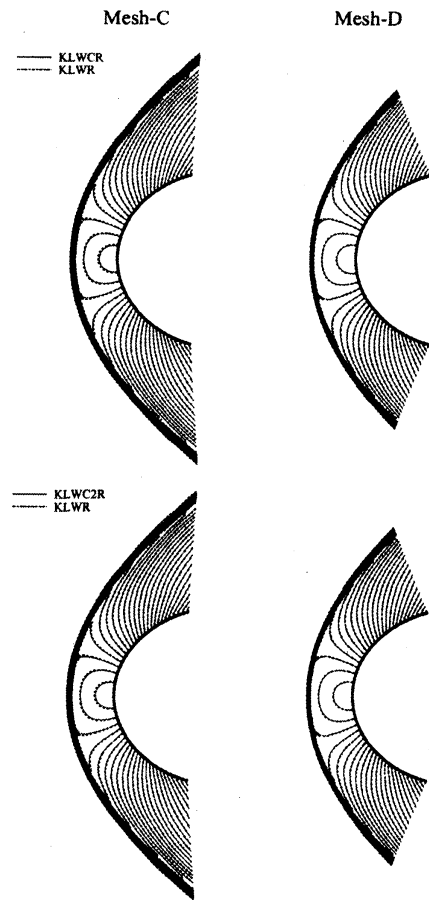


Figure 2: Density contours.

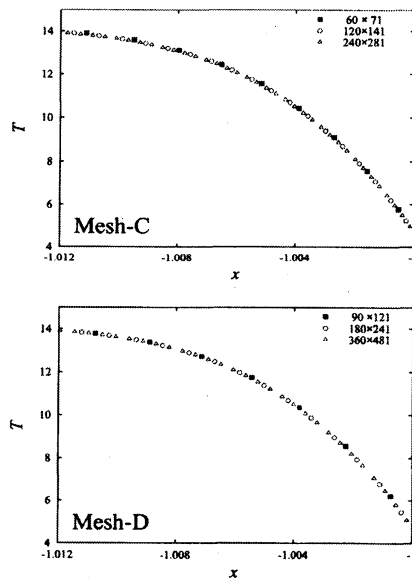


Figure 3: Temperature distribution in the boundary-layer (KLWCR).

References

- [1] B. Einfeldt, "On Godunov-type methods for gas dynamics", *SIAM J. Numer. Anal.* **25** (2), 294-318 (1988).
- [2] A. Harten, P.D. Lax, B. van Leer, "On upstream differencing and Godunov-type schemes for hyperbolic conservation laws," *SIAM Review* **25**, 35-61 (1983).
- [3] T. Kato, Private communication.
- [4] A.E. Mattsson and W.J. Rider, "Artificial viscosity: back to the basics," *Int. J. Numer. Meth. Fluids* **77**, 400-417 (2015).
- [5] R.D. Moser, "On the validity of the continuum approximation in high Reynolds number turbulence," *Phys. Fluids* **18** 078105 (2006).
- [6] J. v. Neumann, "Proposal and analysis of a new numerical method for the treatment of hydrodynamical shock problems," vol. VI, *Collected Works* (Pergamon, London).
- [7] J. v. Neumann and R.D. Richtmyer, "A method for the numerical calculation of hydrodynamic shocks," *J. Appl. Phys.* **21**, 232-237 (1950).
- [8] T. Ohwada and S. Fukata, "Simple derivation of high-resolution schemes for compressible flows by kinetic approach," *J. Comput. Phys.* **211** 424-447 (2006).
- [9] T. Ohwada, R. Adachi, K. Xu, and J. Luo, "On the remedy against shock anomalies in kinetic schemes," *J. Comput. Phys.* **255** 106-129 (2013).
- [10] S. Osher and F. Solomon, "Upwind difference schemes for hyperbolic systems of conservation laws," *Math. Comp.* **38** (158) 339-374 (1982).
- [11] D.I. Pullin, "Direct simulation methods for compressible inviscid ideal-gas flow," *J. Comput. Phys.* **34**, 231-244 (1980).
- [12] R.D. Richtmyer, "Proposed numerical method for calculation of shocks," *Technical Report LA-671*, Los Alamos Scientific Laboratory, Los Alamos, New Mexico, USA, 1948 (available from <http://lib-www.lanl.gov/cgi-bin/getfile?00329037.pdf>).
- [13] R.D. Richtmyer, "Proposed numerical method for calculation of shocks, II," *Technical Report LA-699*, Los Alamos Scientific Laboratory, Los Alamos, New Mexico, USA, 1948 (available from <http://lib-www.lanl.gov/cgi-bin/getfile?00423522.pdf>).
- [14] V.V. Rusanov, "The calculation of the interaction of non-stationary shock waves and obstacles," *USSR Comput. Math. Math. Phys.* **1**(2), 304-320 (1962); *Zh. vych. mat.* **1**: No. 2, 267-279 (1961).
- [15] Y. Shibata, Private communication.
- [16] E.F. Toro, M. Spruce, and W. Speares, "Restoration of the contact surface in the HLL-Riemann solver," *Shock Waves* **4**, 25-34 (1994).
- [17] K. Xu, "A gas-kinetic BGK scheme for the Navier-Stokes equations and its connection with artificial dissipation and Godunov method," *J. Comput. Phys.* **171**, 289-335 (2001).